Reprinted from "The Indian Concrete Journal", May 1964.

UPPER BOUNDS FOR COLLAPSE LOADS OF CYLINDRICAL SHELLS

by N. V. RAMAN and M. N. KESHAVA RAO*

The upper bounds for collapse loads of cylindrical shells with edge beams of different rigidities are obtained by using the limit analysis theory. Three velocity fields are considered to cover different modes of failure. Typical values for the upper bounds are given in a table and are also shown in the form of graphs. Similar graphs can be easily prepared for various parameters of shape and size of the cylindrical shell.

METHODS of limit analysis are being increasingly used to determine the collapse loads of structures. A number of methods are available to estimate the loads causing failure of structures such as continuous beams, rigid frames, arches, plates and slabs with different boundary conditions. For many of these the analysis is easily applied and exact collapse loads can be found. For others the formulation becomes complicated and, in certain cases, impossible. In such cases it is usual to look for upper and lower bounds for the collapse load. Such bounds have been obtained only for a few simple structural shapes. Very little work has been done on the application of methods of limit analysis to shell structures other than shells of revolution. Fialkow appears to be the first to give upper and lower bounds for the collapse loads of partial circular cylindrical shells supported at the ends on diaphragms.[1] In practical shell roof structures cylindrical shells are rarely without edge beams. Baker and Johansen have given methods of obtaining upper bounds for the collapse loads of cylindrical shells with edge beams ; but, they assume the whole structure to be a simple beam for the analysis.[2,3] Hence their estimates can be good only for long shells with weak edge beams. Sawczuk reports tests to distruction of some shells and only indicates a possible approach to determine the bounds, leaving the real problem unsolved.[4]

In this article a method to obtain good upper bounds for collapse loads of cylindrical shells with edge beams is presented. A method to obtain lower bounds has been given in a previous paper.[6]

Generalized stress resultants, yield surface, flow law, and strain rate vectors

In the analysis presented here, it is assumed that the material is isotropic and homogeneous ; the stress-strain diagram is that of a rigid-plastic material ; the Von-Mises yield condition represents the initiation of plastic flow of the material ; the uniform thick shell can be replaced by a sandwich shell.

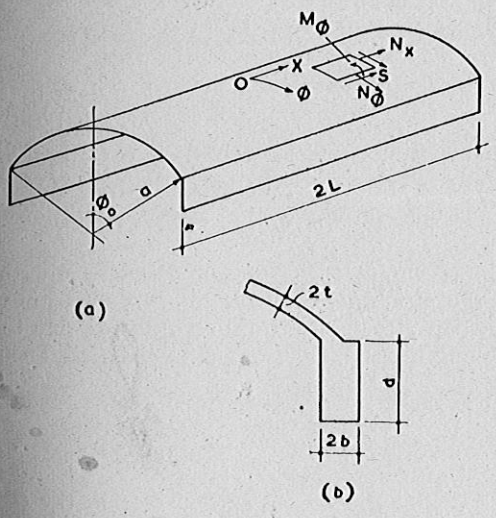

Fig 1

Fig 1 shows the positive direction of the forces N_x, N_ϕ, S, and $M\phi$. The moment acting on a shell element along the x direction is neglected. The radial shear force is not considered as a generalised stress resultant, as the work done by this force is negligible. The linear approximation to the Von-Mises yield condition for stresses σ_x and σ_ϕ expressed in terms of the generalised non-dimensional stress resultants n_x, n_ϕ, s and m results in a yield polyhedron bounded by planes as given below.[1]

Face	*Equations* $f_i = O$
A	$n_x - n_\phi - m = 1$
B	$-n_\phi - m = 1$
C	$-n_x + n_\phi - m = 1$
D	$n_x - n_\phi + m = 1$
E	$-n_\phi + m = 1$
F	$-n_x + n_\phi + m = 1$
G	$n_\phi - m = 1$
H	$n_\phi + m = 1$
J	$n_x = 1$
K	$-n_x = 1$
L	$s = 1$
M	$-s = 1$

If u, v and w are the displacements along x, ϕ and normal directions respectively, then the corresponding non-dimensional strain rate vector components $\dot{\varepsilon}_x$, $\dot{\varepsilon}_\phi$, $\dot{\gamma}$ and $H\dot{\chi}$ for a given velocity field (U, V, W) are obtained from

$$\dot{\varepsilon}_x = \frac{\partial U}{\partial x} \qquad \dot{\gamma} = \left(\frac{1}{r}\frac{\partial U}{\partial \phi} + \frac{r}{\partial x}\frac{\partial V}{\partial x} \right),$$

$$\dot{\varepsilon}_\phi = \left(\frac{\partial V}{\partial \phi} - W \right), \; H\dot{\chi} = -h\left(\frac{\partial^2 W}{\partial \phi^2} + \frac{\partial V}{\delta \phi} \right) \quad .. \quad (1)$$

where $U = \frac{u}{L}$, $V = \frac{v}{a}$ and $W = \frac{w}{a}$ .....(2)

The strain rate vectors are related to the generalised stresses through the flow law [7]

$$\dot{\varepsilon}_x = \lambda_i \frac{\partial f_i}{\partial n_x} \quad .....(a)$$

$$\dot{\varepsilon}_\phi = \lambda_i \frac{\partial f_i}{\partial n_\phi} \quad .....(b) \quad .....(3)$$

$$\dot{\gamma} = \lambda_i \, \partial f_i / \partial s \quad .....(c)$$

$$\text{and } H\dot{\chi} = \lambda_i \, \partial f_i / \partial m \quad .....(d)$$

where $f_i = O$, is the yield surface, representing the faces A, B, C etc., and λ_i are positive constant coefficients. The

* Senior and Junior Scientific Officers, respectively, the Central Building Research Institute, Roorkee.

NOTATION

B	Nondimensional breadth factor for edge beam $= \frac{t}{b}$
D	Nondimensional depth factor for edge beam $= \frac{d}{a}$
E	External energy
$A,B,\ldots L,M,$	Faces of the yield polyhedron
I	Internal energy
J	A constant $= \cos\phi_1$
K_1, K_2	Constants
$2L$	Length of the shell
P	Nondimensional collapse load factor $= \frac{pa}{2\sigma_0 t}$
U	Nondimensional displacement factor in x direction $= \frac{u}{L}$
V	Nondimensional displacement factor in ϕ direction $= \frac{v}{a}$
W	Nondimensional displacement factor in radial direction $= \frac{w}{a}$
X	Distance from O in x direction
Z	Distance measured along the depth of the edge beam positive downwards from the top of the edge beam
a	Radius of the shell
$2b$	Breadth of the edge beam
d	Depth of the edge beam
h	Nondimensional thickness factor $= \frac{t}{2a}$
m	Nondimensional moment factor $= \frac{M_\phi}{\sigma_0 t^2}$
n_x	Nondimensional force factor in x direction $= \frac{Nx}{2\sigma_0 t}$
n_ϕ	Nondimensional force factor in ϕ direction $= \frac{N_\phi}{2\sigma_0 t}$
p	Uniformly distributed load per unit area of shell surface
r	Nondimensional radius parameter $= \frac{a}{L}$
s	Nondimensional shear force factor $= \frac{S}{2\sigma_0 t}$
$2t$	Thickness of shell
u	Displacement of the shell in x direction
v	Displacement of the shell in ϕ direction
w	Displacement of the shell in radial direction
x	Nondimensional coordinate distance in x direction $= \frac{X}{L}$
z	Nondimensional coordinate distance measured along the depth of the edge beam from top of the edge beam $= \frac{Z}{a}$
σ_x	Stress per unit area in x direction
σ_ϕ	Stress per unit area in ϕ direction
σ_o	Yield stress of the material
$\tau_{x\phi}$	Shear stress per unit area
ϕ_o	Semi central angle of the cylindrical shell
ϕ	Angle measured along ϕ direction
$\psi, \theta, \mu, \phi_1, \phi_3, \phi_4$	Angle parameters
ε_x	Nondimensional strain factor in x direction
ε_ϕ	Nondimensional strain factor in ϕ direction
γ	Nondimensional shear strain factor in x-ϕ direction
α	Rotation of a portion of shell
β	Angle subtended at the centre by the axis of rotation
δ	Nondimensional vertical displacement factor $= \Delta/a$
Δ	Vertical displacement
$H\varkappa$	Nondimensional curvature factor in ϕ direction

flow law, in other words, simply states that during plastic flow of the material associated with a yield state of stress, the strain rate vector must lie on the outward normal to the yield surface at a point on the surface corresponding to the given yield state of stress.[7] If the yield surface consists of a number of intersecting planes, as in the present case, then the strain rate vector is normal to that plane which represents the stress state of the point under consideration, and points outwards. If the stress point lies on an intersection of two planes or on a vertex, then the strain rate vector must lie between the outward normals to several intersecting planes.

A kinematically admissible velocity field is one which satisfies the following conditions :

(*a*) It must satisfy the velocity constraints on the structure ; namely the continuity requirements and boundary conditions.

(*b*) The total external rate of work E done by the actual loads P on the proposed velocities is positive.

(*c*) The strains vanish everywhere except on yield lines.

It may be seen that certain discontinuities in the velocities are permissible provided the above conditions are not violated.

The upper bound P is then obtained by equating I, the total energy rate, due to all the internal forces in the structure at collapse to E, the total energy rate due to external loads moving through the proposed velocities. Then,

$$I = 2\sigma_0 tLa \iint (n_x \dot{\varepsilon}_x + n_\phi \dot{\varepsilon}_\phi + \frac{s}{\sqrt{3}}\dot{\gamma} + mH\dot{\varkappa})\,d\phi\,dx \quad \ldots\ldots\ldots (5)$$

$+$ energy rate in the edge beam

$$E = 2\sigma_0 tLa \iint P\,\delta\,d\phi\,dx \quad \ldots\ldots\ldots\ldots\ldots (6)$$

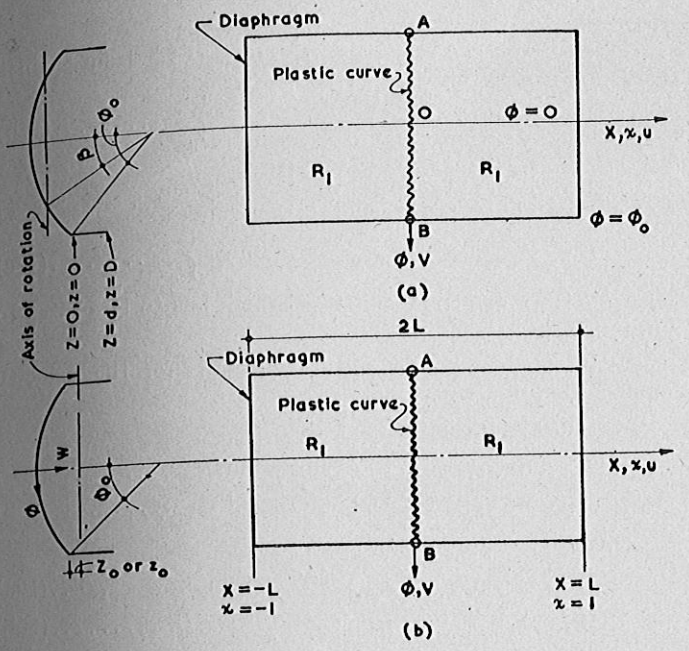

Fig 2

and for uniform loading

$$P = \frac{I}{2\sigma_o tLa \int\int \delta d\phi dx} \quad \ldots\ldots\ldots\ldots\ldots\ldots\ldots\ldots (7)$$

If a partly arbitrary velocity field is selected such that it is kinematically admissible and the expression for P is minimised to P_u by varying the field, then P_u is a good upper bound for the collapse load.

Kinematically admissible velocity fields and upper bounds

Only three velocity fields are considered in this paper and the upper bound P_u is found as the lowest of the P's given by the three fields.

Velocity field I

The velocity field I is selected so as to correspond to the displacement pattern of a simply supported beam at collapse. At $x = O$, a plastic curve (or yield line) AB separates two rigid portions R_1. In the first case the rotation of R_1 is about a horizontal axis passing through $\phi = \pm \beta$ at the ends of the shell (*Fig 2a*). In the second case, (*Fig 2b*), the axis of rotation is taken to pass through the edge beams at the ends of the shell.

The first case is applicable to shells having shallow edge beams, and the second case to shells with deep edge beams.

Case (i), when the axis of rotation passes through $\phi = \pm\beta$ (*Fig 2a*): With the displacement pattern symmetrical about $\phi = O$ and $x = O$, the quarter shell $O<\phi<\phi_0$, $O<x<1$ is typical and the displacement field in region R_1 is given by

$$U = \alpha r(\cos\beta - \cos\phi) \text{ in the shell, } O<\phi<\phi_0 \ldots (8a)$$
$$U = \alpha r\ (\cos\beta - \cos\phi_o + z) \text{ in the edge beam, } O<z<D, \ \ldots\ldots\ldots\ldots\ldots\ldots\ldots\ldots (8b)$$

$$V = \frac{\alpha}{r}(1 - x)\sin\phi, \quad \ldots\ldots\ldots\ldots\ldots\ldots\ldots\ldots (8c)$$

and $$W = \frac{\alpha}{r}(1 - x)\cos\phi \quad \ldots\ldots\ldots\ldots\ldots\ldots\ldots\ldots (8d)$$

It may be easily verified that the above displacement field satisfies the boundary conditions, namely, $V = W = O$ at $x = 1$ and W is continuous throughout. The rigid body nature of the displacements in the region R_1 is also easily verified by the fact that the strains $\varepsilon_x = \varepsilon_\phi = H\varkappa = \gamma = O$. The velocity field corresponding to the displacements (8) is, therefore, kinematically admissible. The discontinuity in U gives rise to a strain in the direction x along the plastic curve AB. As discontinuities in V and W do not exist along AB, the strains due to these are zero. The internal energy, therefore, is only that due to ε_x. Denoting a discontinuity in U by $U]$, we have

$$U]_{shell} = \alpha r\ (\cos\beta - \cos\phi)$$
$$U]_{beam} = \alpha r\ (\cos\beta - \cos\phi_o + z)$$

Then, $U]_{shell} \leq O$ for $O<\phi<\beta$

$U]_{shell} \geqq O$ for $\beta<\phi<\phi_o$

and $U]_{beam} > O$ for $O<z<D$

The applicable plastic regimes for the strain ε_x corresponding to the above discontinuities (selected from the table on page 172) are :

$$n_x = -1, \qquad O\leq\phi\leq\beta$$
$$n_x = +1, \qquad \beta\leq\phi\leq\phi_o \text{ and } O<z<D.$$

Then, from equation (5), the internal energy in the typical quarter shell due to $n_x = \pm 1$ and ε_x may be written as

$$I = 2\sigma_o tLa\left[\int_0^\beta (-1)\alpha r(\cos\beta - \cos\phi)\, d\phi + \int_\beta^{\phi_o} (+1)(\alpha r)(\cos\beta - \cos\phi)\, d\phi + \frac{1}{B}\int_0^D (+1)(\cos\beta - \cos\phi_o + z)\alpha r\, dz\right]$$

$$= 2\sigma_o tLa\alpha r\left\{\phi_o\cos\beta - \sin\phi_o - 2\beta\cos\beta + 2\sin\beta + (\cos\beta - \cos\phi_o)\frac{D}{B} + \frac{D^2}{2B}\right\} \ldots\ldots\ldots\ldots (9)$$

From equation (6), the external energy in the quarter shell due to the vertical loading of p per unit area of shell surface is

$$E = 2\sigma_o tLa\, P \int_0^{'} \int_0^{\phi_o} \delta d\phi dx$$

where δ = vertical deflection $= \frac{\alpha}{r}(1-x)$ from equation (8)

Hence $$E = 2\sigma_o tLa\, P\, \frac{\alpha}{r}\, \frac{\phi_o}{2} \quad \ldots\ldots\ldots\ldots\ldots\ldots\ldots\ldots (10)$$

Equating equations (9) and (10),

$$P = 2r^2/\phi_o \left\{\phi_o\cos\beta - \sin\phi_o - 2\beta\cos\beta + 2\sin\beta + (\cos\beta - \cos\phi_o)\frac{D}{B} + \frac{D^2}{2B}\right\} \ldots\ldots\ldots\ldots\ldots (11)$$

For P to be minimum, $$\beta = \frac{1}{2}\left\{\phi_o + \frac{D}{B}\right\} \quad \ldots\ldots\ldots (12)$$

P_u, the upper bound for the displacement field (8) is then given by equations (11) and (12).

Case (ii), when the axis of rotation passes through the edge beam (*Fig 2b*): The displacement field (8) gets altered only in U

$$U = \alpha r\ (\cos\phi_o - z_o - \cos\phi) \text{ for } O<\phi<\phi_o \ldots (13a)$$
$$U = \alpha r\ (z - z_o) \text{ for } O<z<D \ \ldots\ldots\ldots\ldots\ldots (13b)$$

Equations (13a) and (13b) along with (8c) and (8d) define the displacement pattern for the velocity field shown in *Fig* 2 (b). The only discontinuity is in U and is given by

$U] = \alpha r \quad (\cos\phi_o - z_o - \cos\phi)$ and is $<O$, in $O<\phi<\phi_o$

$U] = \alpha r\,(z - z_o)$ and is $<O$, in $O<z<z_o$

$U] = \alpha r\,(z - z_o)$ and is $>O$ in $z_o<z<D$

As before, the applicable plastic regimes corresponding to the above mentioned discontinuities are

$n_x = -1$ in $O<\phi<\phi_o$ and in $O<z<z_o$

$n_x = +1$ in $z_o<z<D$.

From (5) the internal energy due to these forces and discontinuities may be written down as before.

$$I = 2\sigma_o t L a \alpha r \left\{ \sin\phi_o - \phi_o \cos\phi_o + \phi_o z_o + \frac{z_o^2}{B} + \frac{D^2}{2B} - \frac{z_o D}{B} \right\} \quad \ldots\ldots\ldots(14)$$

External energy E remains the same as in equation (10).

From equations (14) and (10), $P = \dfrac{2r^2}{\phi^o}\left\{ \sin\phi_o - \phi_o\cos\phi_o + \phi_o z_o + \dfrac{z_o^2}{B} - \dfrac{z_o D}{B} + \dfrac{D^2}{2B} \right\}$

P is minimised by chosing $z_o = \frac{1}{2}\left\{ D - B\phi_o \right\}$

Then P_u, the upper bound for case (ii), may be found as

$$P_u = \frac{2r^2}{\phi_o}\left\{ \sin\phi_o - \phi_o\cos\phi_o - \frac{B\phi_o^2}{2} + \frac{1}{4B}(D + B\phi_o)^2 \right\} \quad \ldots\ldots\ldots(15)$$

Velocity field II

Consider an yield pattern as shown in *Fig* 3. The right portions R_1 and R_2 are separated by a curved yield line EB. It is assumed here that the edge beams are very strong and the failure is taking place because of yielding in the shell. The shell separates itself from the edge beam forming a plastic hinge and becomes a mechanism.

Consider a velocity field corresponding to the following displacement pattern.

In region R_1,

$$U = \alpha r(J - \cos\phi) \quad \ldots\ldots\ldots(16a)$$

$$V = \frac{\alpha}{r}(1 - x)\sin\phi \quad \ldots\ldots\ldots(16b)$$

and $W = \dfrac{\alpha}{r}(- - x)\cos\phi \quad \ldots\ldots\ldots(16c)$

In region R_2,

$$U = 0 \quad \ldots\ldots\ldots(17a)$$

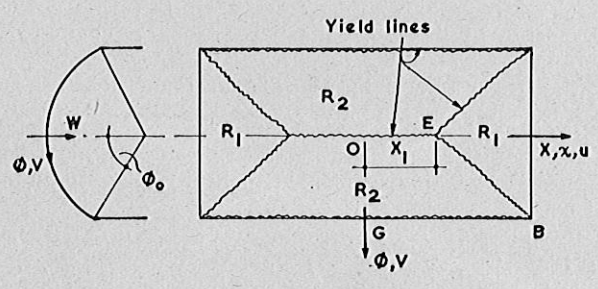

Fig 3

$$V = \frac{\alpha}{r}(1 - x_1)\operatorname{cosec}\phi_0 \left\{ \cos\phi_0\cos\phi + \sin\phi_0\sin\phi - 1 \right\} \quad \ldots\ldots\ldots(17b)$$

$$W = \frac{\alpha}{r}(1 - x_1)\operatorname{cosec}\phi_0 \left\{ \cos\phi\sin\phi_0 - \cos\phi_0 \sin\phi \right\} \quad \ldots\ldots\ldots(17c)$$

where J is an arbitrary constant which has to be chosen to minimise P.

The boundary and continuity conditions for the velocity field are as follows :

Boundary conditions :

$V = W = 0$ at $\phi = \phi_0$ in region R_2 $\ldots\ldots\ldots(18a)$

$V = W = 0$ at $x = 1$ in region R_1 $\ldots\ldots\ldots(18b)$

Continuity conditions :

W_{R_2} is continuous along $\phi = 0$ in $o<x<x_1$ $\ldots(19a)$

$W_{R_1} = W_{R_2}$, along the yield line EB $\ldots\ldots\ldots(19b)$

It may be easily verified that the velocity field corresponding to equations (16) and (17) satisfies the requirements of equations (18) and (19). It may also be verified that the conditions for rigid body motion are also satisfied. The velocity field shown in *Fig* 3 is, therefore, kinematically admissible.

The equation of the yield curve satisfying equations (16), (17), and (19) is

$$(x - x_1) = (1 - x_1)\cot\phi_0\tan\phi \quad \ldots\ldots\ldots(20a)$$

which on differentiation gives

$$dx = (1 - x_1)\cot\phi_0\sec^2\phi d\phi \quad \ldots\ldots\ldots(20b)$$

Yield line OE

Discontinuities along $\phi = 0$ are

$$U \Big] = 0$$

$$V \Big] = \frac{\alpha}{r}(1 - x_1)\operatorname{cosec}\phi_0(\cos\phi_0 - 1)$$

$$\frac{\partial W}{\partial\phi} \Big] = -\frac{\alpha}{r}(1 - x_1)\operatorname{cosec}\phi_0\cos\phi_0$$

It is seen that ε_x and γ corresponding to the above discontinuities are zero. From the above, it may be seen that the strain rate vector component $\dot{\varepsilon}_\phi$ is always negative and $H\dot{\varkappa}$ is always positive. $(\dot{\varepsilon}_\phi + H\dot{\varkappa})$ is negative provided $h < (1 - \cos\phi_0)$. This condition is always satisfied in practice. A stress state for the strain rate vector mentioned above is next selected. The selection of the face of the yield polyhedron should be such that $\dot{\varepsilon}_\phi$ is always negative, $H\dot{\varkappa}$ is always positive $(\dot{\varepsilon}_\phi + H\dot{\varkappa})$ is always negative and $\dot{\varepsilon}_x = \gamma = 0$. From the equations of the faces of the polyhedron given on the table on page 172, the only intersection satisfying these conditions is between the faces B and E given by

$-m - n_\phi = 1 \ldots\ldots B$

$+m - n_\phi = 1 \ldots\ldots E$

The intersection of the faces B and E gives $n_\phi = -1$ and $m = 0$. From equation (5), the internal energy along the yield line OE is

$$I_{OE} = 2\sigma_o t L a \int_0^{x_1} (-1)\frac{\alpha}{r}(1 - x_1)\operatorname{cosec}\phi_o(\cos\phi_o - 1)dx$$

$$= 2\sigma_o t L a \left\{ \frac{\alpha}{r}(1 - x_1)x_1\operatorname{cosec}\phi_0(1 - \cos\phi_0) \right\} \quad \ldots\ldots(21)$$

Yield line GB

Discontinuities along $\phi = \phi_0$

$$\left.\begin{matrix} U \\ V \\ W \\ \frac{\partial W}{\partial \phi} \end{matrix}\right] = 0, \quad 0, \quad 0, \quad -\frac{\alpha}{r}(1 - x_1)\operatorname{cosec}\phi_0$$

All the strains ε_x, ε_ϕ, γ are zero excepting $H\dot{\varkappa}$. $H\dot{\varkappa}$ corresponding to the discontinuity in $\frac{\partial W}{\partial \phi}$ is always positive and the corresponding stress state can be easily selected as $m = +1$. The internal energy along the yield line GB can be now written as

$$I_{GB} = 2\sigma_0 tLa \left\{ \frac{h\alpha}{r}(1 - x_1)\operatorname{cosec}\phi_0 \right\} \quad \ldots\ldots\ldots (22)$$

Yield line EB

The equation for the curved yield line EB from equation (20) is $(x - x_1) = (1 - x_1)\cot\phi_0 \tan\phi$. To determine the discontinuities in the coordinate directions, it is necessary to find the normal jumps across the yield line EB.[5] The jumps in the displacements U, V and W in the direction N (*Fig* 4) are given by

$$U]_N = \alpha r(J - \cos\phi)$$

$$V]_N = \frac{\alpha}{r}(1 - x_1)\operatorname{cosec}\phi_0 (1 - \sec\phi\cos\phi_0)$$

$$\left.\frac{\partial W}{\partial \phi}\right]_N = \frac{\alpha}{r}(1 - x_1)\operatorname{cosec}\phi_0 \cos\phi_0 \sec\phi$$

The jumps in the coordinate directions x and ϕ are

$$U]_x = \alpha r(J - \cos\phi)\cos\psi,$$

$$U]_\phi = \alpha r(J - \cos\phi)(-\sin\psi),$$

$$V]_\phi = \frac{\alpha}{r}(1 - x_1)\operatorname{cosec}\phi_0 (1 - \sec\phi\cos\phi_0)(-\sin\psi),$$

$$V]_x = \frac{\alpha}{r}(1 - x_1)\operatorname{cosec}\phi_0 (1 - \sec\phi\cos\phi_0)\cos\psi,$$

$$\left.\frac{\partial W}{\partial \phi}\right]_x = \frac{\alpha}{r}(1 - x_1)\operatorname{cosec}\phi_0 \cos\phi_0 \sec\phi \cos\psi,$$

and $$\left.\frac{\partial W}{\partial \phi}\right]_\phi = \frac{\alpha}{r}(1 - x_1)\operatorname{cosec}\phi_0 \cos\phi_0 \sec\phi\,(-\sin\psi).$$

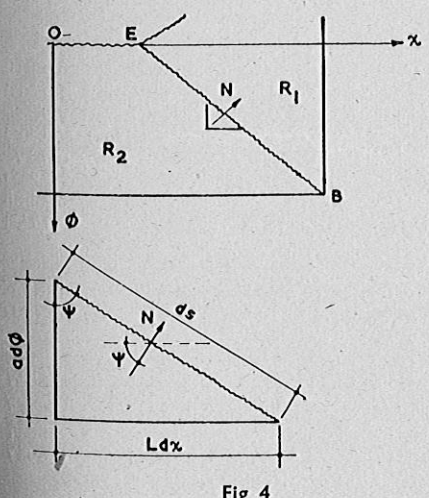

Fig 4

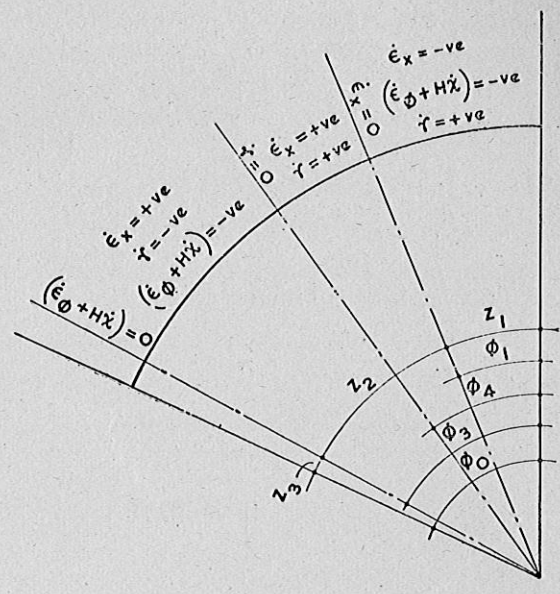

Fig 5

Replacing J by $\cos\phi_1$ where $\phi_1 < \phi_0$, the signs of the strain rate vector components corresponding to the above discontinuities may be written down from equation (1) (*Fig* 5).

$\dot{\varepsilon}_x$ is $-ve$ in $O < \phi < \phi_1$, Zone Z_1

$\dot{\varepsilon}_x$ is $+ve$ in $\phi_1 < \phi < \phi_0$

$\dot{\varepsilon}_\phi$ is $-ve$ in $O < \phi < \phi_0$

$H\dot{\varkappa}$ is $+ve$ in $O < \phi < \phi_0$

$(\dot{\varepsilon}_\phi + H\dot{\varkappa})$ is $-ve$ in $O < \phi < \phi_3$

$(\dot{\varepsilon}_\phi + H\dot{\varkappa})$ is $+ve$ in $\phi_3 < \phi < \phi_0$, Zone Z_3,

$\dot{\gamma}$ is $+ve$ in $O < \phi < \phi_4$

$\dot{\gamma}$ is $-ve$ in $\phi_4 < \phi < \phi_0$,

where $$\cos\phi_3 = \frac{\cos\phi_0}{1 - h} \quad \ldots\ldots\ldots\ldots\ldots\ldots (23)$$

and $$\sec\phi_4 = \sqrt{(\sec\phi_0 \sec\phi_1)} \quad \ldots\ldots\ldots\ldots (24)$$

Vertices or intersections of planes on the surface of the yield polyhedron representing the stress state to give the strain rate vectors corresponding to the discontinuities discussed above may be found so that the stresses satisfy the flow law (3).

For Zone Z_1, $O < \phi < \phi_1$, the point on the surface of the yield polyhedron with the coordinates $n_x = -1$, $s = +1$, $n\phi = -1$ and $m = 0$, satisfies the requirements of the flow law for the strain rate vector $(\dot{\varepsilon}_x, \varepsilon_\phi \dot{\gamma}, H\dot{\varkappa})$.

For Zone Z_2, $\phi_1 < \phi < \phi_3$, two points on the surface of the yield polyhedron satisfy the flow law. The strain rate vector component $\dot{\gamma}$ is, however, independent and the energy due to shear s is determined separately. The two points on the yield surface satisfying the flow law for the strain rate vector $(\varepsilon_x, \varepsilon\phi, H\dot{\varkappa})$ are $n_x = O, n\phi = -1, m = +1$ and $n_x = +1$, $n\phi = O$, $m = O$.

As h is a small quantity, $\phi_3 \approx \phi_0$ from equation (23) and hence zone Z_3 need not be considered. The energies in these different zones may now be written using equation (5):

$$Iz_1 = 2\sigma_0 tLa \left[\alpha r \int_0^{\phi_1} (\cos\phi_1 - \cos\phi)(-1)d\phi \right.$$

$$\left. + \int_{x1}^{1} (-1)(-)\frac{\alpha}{r}(1 - x_1)\operatorname{cosec}\phi_0 (1 - \sec\phi\cos\phi_0)dx \right]$$

$$= 2\sigma_o tLa \left[\alpha r(\sin\phi_1 - \phi_1\cos\phi_1) + \frac{\alpha}{\gamma}(1-x_1)^2 \operatorname{cosec}\phi_o \cot\phi_o \left\{ \tan\phi_1 - \frac{\cos\phi_o}{2}(\sec\phi_1\tan\phi_1 + \log\sec\phi_1 + \tan\phi_1) \right\} \right]$$

Iz_2 due to $n_x = +1$, $n\phi = O$, $m = O$, results in

$$Iz_2a = 2\sigma_o tLa \int_{\phi_1}^{\phi_o} \alpha r(\cos\phi_1 - \cos\phi)\, d\phi$$

$$= 2\sigma_o tLa \left[\alpha r \left\{ \cos\phi_1(\phi_o - \phi_1) - (\sin\phi_o - \sin\phi_1) \right\} \right] \quad \ldots\ldots(26a)$$

Iz_2b, due to $n_x = O$, $n\phi = -1$, $m = +1$, results in $Iz_2b =$

$$2\sigma_o tLa \frac{\alpha}{\gamma}(1-x_1)^2 \operatorname{cosec}\phi_o \cot\phi_o \left[(\tan\phi_o - \tan\phi_1)(1+h) - \frac{\cos_o\phi}{2} \left\{ \sec\phi_o\tan\phi_o - \sec\phi_1\tan\phi_1 + \log\frac{\sec\phi_o + \tan\phi_o}{\sec\phi_1 + \tan\phi_1} \right\} \right] \quad \ldots\ldots(26b)$$

Energy due to $\dot\gamma$, I_γ is

$$I_\gamma = 2\sigma_o tLa \left[\alpha(1-x_1)\operatorname{cosec}\phi_o \int_o^{\phi_4} \frac{(1)}{\sqrt{3}}(1 - \cos\phi_o\cos\phi_1\sec^2\phi)d\phi + \alpha(1-x_1)\operatorname{cosec}\phi_o \int_{\phi_4}^{\phi_o} \frac{(-1)}{\sqrt{3}}(1 - \cos\phi_o\cos\phi_1\sec^2\phi)d\phi \right]$$

$$= 2\sigma_o tLa \frac{\alpha}{\sqrt{3}}(1-x_1)\operatorname{cosec}\phi_o [2\phi_4 - \phi_o - 2\cos\phi_o\cos\phi_1\tan\phi_4 + \sin\phi_o\cos\phi_1] \quad \ldots\ldots(27)$$

where ϕ_4 is as defined in equation (24).

Total internal energy for the quarter shell, $O < \phi < \phi_o$, $O < x < 1$ may now be written as

$$Ia = Iz_1 + Iz_2a + I\dot\gamma + I_{OE} + I_{GB} \quad \ldots\ldots(28a)$$

and $$Ib = Iz_1 + Iz_2b + I\dot\gamma + I_{OE} + I_{GB} \quad \ldots\ldots(28b)$$

It can be shown that I_a is less than Ib and for minimum internal energy only I_a is considered in the following discussion.

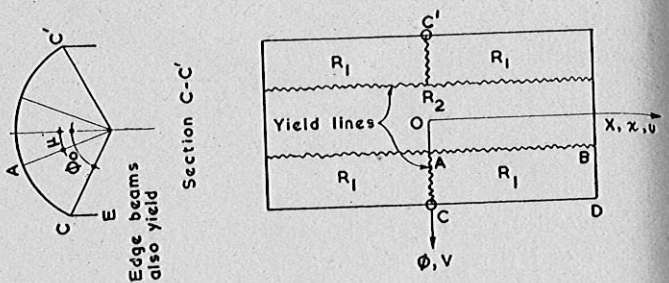

Fig 6

External energy E

From the displacement field (16) and (17), the vertical deflection δ is

$$\delta = \frac{\alpha}{\gamma}(1-x) \text{ in region } R_1 \quad \ldots\ldots(29a)$$

and $$\delta = \frac{\alpha}{\gamma}(1-x_1)\operatorname{cosec}\phi_0(\sin\phi_0 - \sin\phi) \text{ in region } R_2 \quad (29b)$$

Using equations (6) and (20) together with equation (29), the external energy E for the quarter shell $0 < \phi < \phi_0$, $0 < x < 1$, is

$$E = 2\sigma_0 tLa\, P\frac{\alpha}{\gamma}(1-x_1)\operatorname{cosec}\phi_0 \left[\frac{(1-x_1)}{2}\operatorname{cosec}\phi_0 \left\{ \phi_0\sin^2\phi_0 + \cos^2\phi_0(\tan\phi_0 - \phi_0) + 2\cos\phi_0\sin\phi_0 - 2\cos\phi_0\log_e(\sec\phi_0 + \tan\phi_0) \right\} + x_1(\cos\phi_0 + \phi_0\sin\phi_0 - 1) \right] \quad \ldots\ldots(30)$$

Using equations (28) and (30) in equation (7), P is found from

$$E = I_a \quad \ldots\ldots(31)$$

It may be seen that both I_a and E contain arbitrary quantities x_1 and ϕ_1. These quantities should be so chosen as to minimise the value of P resulting from equation (31). The resulting expression for P from equation (31) may be differentiated both with respect to ϕ_1 and with respect to x_1 and equated to zero. These two equations may be solved for ϕ_1 and x_1. In most of the practical problems the value of ϕ_1 to give a turning value of P is greater than ϕ_0. Hence it is sufficient to solve for x_1 only and then to select a value for ϕ_1 to make P minimum. It is found, for a value of $\phi_o = 40°$, that P is minimum for $\phi_1 = 0$ and $x_1 = 0$. The values of P_u given in *Table* 1 correspond to $\phi_1 = 0$ and $x_1 = 0$.

Velocity field III

Consider a yield pattern which is a modification of velocity field I as shown in *Fig* 6.

Table 1 Values of P_u (upper bounds to collapse loads) (corresponding values of μ are given in brackets).

D \ γ	0·2	0·4	0·6	0·8	1·0	1·2	1·4	1·6	1·8	2·0	
0·000	0·0048	0·01869 (5°)	0·0284 (10°)	0·0380 (15°)	0·0475 (17½°)	0·0567 (20°)	0·0661 (22½°)	0·0746 (22½°)	0·0843 (25°)	0·0910 (25°)	Field III
0·025	0·0066	0·02634 (7½°)	0·0439 (12½°)	0·0638 (17½°)	0·0866 (20°)	0·1120 (20°)	0·1383 (22½°)	0·1686 (22½°)	0·2015 (25°)	0·2365 (25°)	
0·050	0·0086	0·0344	0·0665 (12½°)	0·1047 (12½°)	0·1509 (17½°)	0·2059 (20°)	0·2733 (20°)	0·344 (22½°)	0·4273 (22½°)	0·517 (22½°)	
0·075	0·0110	0·044	0·0964 (12½°)	0·1594 (15°)	0·2390 (15°)	0·3350 (17½°)	0·4475 (17½°)	0·5775 (17½°)	0·7255 (17½°)	0·8905 (17½°)	
0·100	0·0132	0·0527	0·1185	0·2106	0·3292	0·4742	0·6450	0·8430	1·068	1·315	Field I
0·150	0·0173	0·0691	0·1554	0·2763	0·4320	0·6220	0·8460	1·105	1·398	1·728	
0·200	0·0214	0·0855	0·1924	0·3420	0·5345	0·7690	1·0460	1·2917	1·5377	1·8047	Field I
0·250	0·0259	0·1038	0·2332	0·4150	0·6485	0·8559	1·0647	1·2917	1·5377	1·8047	
0·300	0·0311	0·1245	0·2800	0·4967	0·6662	0·8559	1·0647	1·2917	1·5377	1·8047	
0·350	0·0369	0·1472	0·3314	0·4967	0·6662	0·8559	1·0647	1·2917	1·5377	1·8047	

For the yield pattern shown in *Fig* 6, R_2 cannot have any displacements. Therefore, for R_2,

$$U = 0 \quad \ldots\ldots (32a)$$

$$V = 0 \quad \ldots\ldots (32b)$$

$$W = 0 \quad \ldots\ldots (32c)$$

Let the displacement field for region R_1 in the shell portion be

$$U = \alpha r \left\{ K_1(\phi-\mu) - \sin(\phi-\mu) + K_2 \right\} \quad \ldots\ldots (32d)$$

$$V = \frac{\alpha(1-x)}{r} \left\{ K_1 - \cos(\phi-\mu) \right\} \quad \ldots\ldots (32e)$$

$$W = \frac{\alpha(1-x)}{r} \sin(\phi-\mu) \quad \ldots\ldots (32f)$$

and in the edge beam

$$U = \alpha r \left\{ K_1(\phi_0-\mu) - \sin(\phi_0-\mu) + K_2 + (K_1 \sin\phi_0 - \sin\mu)z \right\} \quad \ldots\ldots (32g)$$

$$\delta = \frac{\alpha(1-x)}{r} \left\{ K_1 \sin\phi_0 - \sin\mu \right\} \quad \ldots\ldots (32h)$$

where K_1, K_2 and μ are arbitrary constants which are chosen to give minimum P.

The displacement field (32) satisfies the continuity conditions along ACE and AB, namely, $U = 0$, $V = 0$, and $W = 0$ along AB ($\phi = \mu$), and the boundary conditions along BD, namely $V = W = 0$ at $x = 1$. The displacement field (32) also satisfies equation (1) for the rigid body nature of displacements as the strains vanish. The velocity field, corresponding to the above displacement field (32) is, therefore, kinematically admissible.

Yield line AB

Discontinuities along $\phi = \mu$ from equation (32) are,

$$U\big]_\phi = \alpha r K_2, \qquad U\big]_x = 0$$

$$V\Big]_\phi = \frac{\alpha(1-x)}{r}\left[K_1 - 1\right], \qquad V\Big]_x = 0$$

$$W] = 0$$

$$\frac{\partial W}{\partial\phi}\Big]_\phi = \frac{\alpha(1-x)}{r}, \qquad \frac{\partial W}{\partial\phi}\Big]_x = 0$$

The direction of the strain rate vector may now be determined.

From $\dot{\varepsilon}_x = 0$; $\dot{\varepsilon}_\phi$ is $-ve$ for $K_1 < 1$;

$H\dot{\varkappa}$ is $-ve$ and $\dot{\gamma}$ is $+ve$ if K_2 is $+ve$.

Choosing the face $(-m - n_\phi = 1)$ on the yield polyhedron, for minimum internal energy satisfying the strain rate vector and flow law, K_1 should be $\frac{1}{1+h}$. The internal energy corresponding to the above discontinuities may be written as

$$I_{AB} = 2\sigma_0 tLa \left\{ \int_0^1 (-m)(-)h\frac{\alpha}{r} K_1(1-x)dx + \int_0^1 (-n_\phi)\frac{\alpha}{r}(K_1-1)(1-x)dx + \int_0^1 \frac{\alpha K_2}{\sqrt{3}}dx \right\} \quad \ldots\ldots (33)$$

$$= \left\{ \frac{h\,\alpha}{(1+h)2r} + \frac{\alpha K_2}{\sqrt{3}} \right\} 2\sigma_0 tLa \quad \ldots\ldots (34)$$

Yield line AC (shell only)

Discontinuities at $x = 0$ from equation (32) are

$$U\Big]_x = \alpha r \left\{ K_1(\phi-\mu) - \sin(\phi-\mu) + K_2 \right\}$$

$$V\Big]_\phi = V\Big]_x = 0; \qquad U\Big]_\phi = 0$$

$$W\Big]_\phi = W\Big]_x = 0;$$

$$\frac{\delta W}{\delta\phi}\Big] = 0$$

The strain rate vector components $\dot{\varepsilon}_\phi$, $H\dot{\varkappa}$ and $\dot{\gamma}$ corresponding to the above discontinuities are zero. The sign of $\dot{\varepsilon}_x$ depends upon K_2 the arbitrary constant.

If K_2 is defined as

$$K_2 = K_1(\mu-\theta) - \sin(\mu-\theta) \quad \ldots\ldots (35)$$

then for $\mu > \theta$,

$$I_{AC_1} = 2\sigma_0 tLa\alpha r \left\{ K_1 \frac{(\phi_0-\mu)^2}{2} + \cos(\phi_0-\mu) + K_2(\phi_0-\mu) - 1 \right\} \quad \ldots\ldots (36a)$$

provided $K_1 > \dfrac{\sin(\mu-\theta)+\sin(\phi_0-\mu)}{(\mu-\theta)+\sin(\phi_0-\mu)}$ $\quad \ldots\ldots (36b)$

and for $\mu < \theta$,

$$I_{AC_2} = 2\sigma_0 tLa\alpha r \left[K_1 \left\{ \frac{(\phi_0-\mu)^2}{2} - (\theta-\mu)^2 \right\} + \cos(\phi_0-\mu) - 2\cos(\theta-\mu) + 1 + K_2 \left\{ (\phi_0-\mu) + 2(\mu-\theta) \right\} \right] \quad \ldots\ldots (36c)$$

provided $K_1 > \sin(\theta-\mu)/(\theta-\mu)$ $\quad \ldots\ldots (36d)$

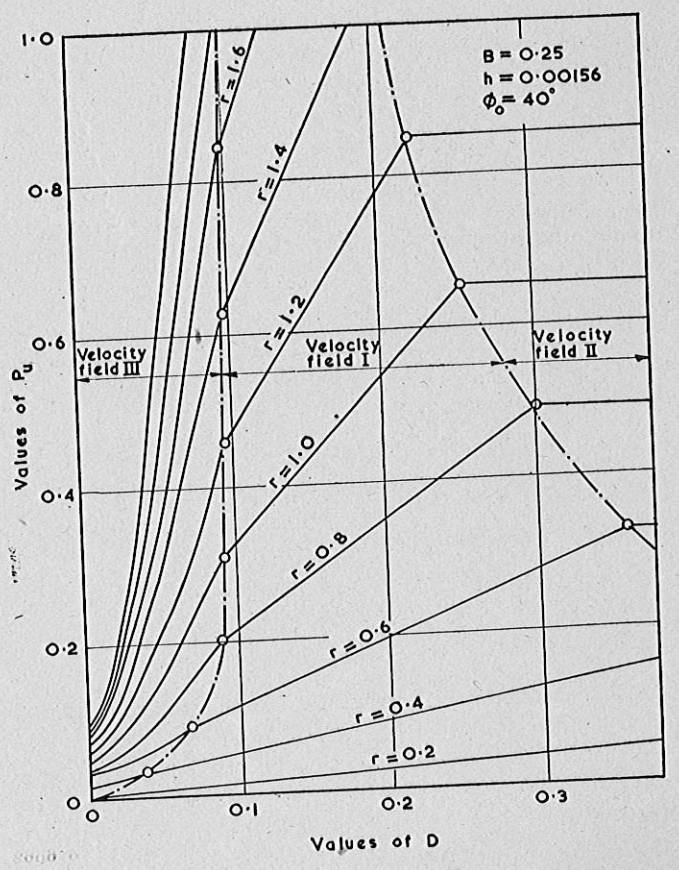

Fig 7

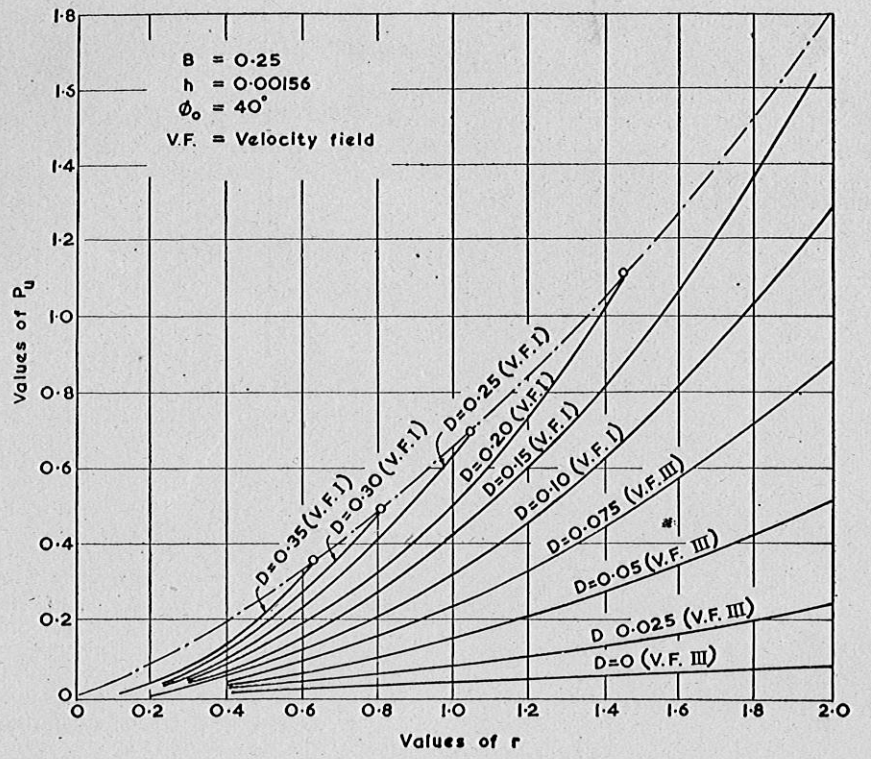

Fig 8

It can be shown that energy for $\mu > \theta$ is always greater than that for $\mu < \theta$ and the latter case alone is considered in the following discussion.

Yield line CE (edge beam portion)

Discontinuities at $x = O$

$$\dot{U}]_x = \alpha r \{K_1(\phi_o - \mu) - \sin(\phi_o - \mu) + (K_1 \sin \phi_o - \sin \mu)z + K_2\}$$

The internal energy corresponding to the above discontinuity may be determined as before.

$$I_{CE} = 2\sigma_o t L a \alpha r \left[\frac{D}{B} \{K_1(\phi_0 - \mu) - \sin(\phi_o - \mu) + K_2\} + \frac{D^2}{2B}(K_1 \sin \phi_o - \sin \mu) \right] \quad \ldots\ldots\ldots (37)$$

The total internal energy in the quarter shell is

$$I = I_{AB} + I_{AC_2} + I_{CE} \quad \ldots\ldots\ldots\ldots\ldots\ldots\ldots (38)$$

External energy

External energy due to the loading p in the quarter shell $O < \phi < \phi_0$, $O < x < 1$, may be found from equation (6).

The vertical deflection

$$\delta = V \sin \phi + W \cos \phi = \frac{\alpha(1-x)}{r}(K_1 \sin \phi - \sin \mu)$$

Then from equation (6),

$$E = 2\sigma_o t L a \frac{P\alpha}{2r} \left\{ K_1(\cos \mu - \cos \phi_0) - (\phi_0 - \mu) \sin \mu \right\} \quad \ldots\ldots\ldots (39)$$

The expression for P may be written by equating E and I and differentiated with respect to μ and θ; these may be found to make P minimum. The values of μ and θ should satisfy the inequality (36d).

Discussion

Table 1 gives the values for the upper bounds for various parameters of shape of shell and size of edge beam. The upper bound Pu is plotted against the non-dimensional radius to length parameter for various values for D in *Figs* 7 and 8. The upper bounds given in *Table* 1 and plotted in *Figs* 7 and 8 are worked out for a value of $\phi_0 = 40°$, $B = 0{\cdot}25$ and $h = 0{\cdot}00156$. *Figs* 7 and 8 are drawn to show the variation of the upper bound with r and D. For other values of ϕ_0, B, and h, the upper bounds may be worked out from the equations derived earlier.

It can be seen from *Fig* 7 that for values of r less than unity and for shallow edge beams the velocity field I (the beam mechanism) gives larger values for Pu than those from the velocity field III. The increase in Pu value with the increase in D is marked especially when r is greater than unity (i.e., for short shells). The region in which the velocity field I holds good is clearly shown in *Fig* 7.

Beyond a certain limiting value for D, any increase in depth of edge beam does not increase the strength of the shell. The failure takes place entirely within the shell. This limiting value for D is found from velocity field II. This value is usually so large that failure in most cases takes place when both edge beam and shell yield.

Though other velocity fields may also exist, excepting for very short shells, the velocity fields considered here fairly well represent the usual failures. The upper bounds given here, however, are not to be mistaken for the actual failure loads. These lie in between the lower bound and the upper bound. To estimate the collapse load it is essential to carry out both lower bound analysis and upper bound analysis. For long and intermediate shells a previous paper explains the lower bound analysis.[6]

The upper bound analysis presented here is for an isotropic and homogeneous material, as is assumed in the elastic analysis of shell structures. The material is also assumed to obey the Von-Mises yield condition. It is not known how far this yield condition which was primarily put forth for metals can be modified for reinforced concrete. Further experimental investigation on reinforced concrete structures to study their behaviour at yield with the specific intention of evolving a

yield condition similar to the Von-Mises yield condition is necessary.

The method outlined is applicable for any yield condition other than Von-Mises. A yield condition for reinforced concrete can as well be used when this becomes available. Perhaps this may increase the complexity of the problem because of the increase in the number of parameters such as areas of steel in coordinate directions, etc. But the procedure remains the same.

Illustrative example

Shell dimensions

$2L = 100$ ft $\qquad B = \frac{t}{b} = 0{\cdot}03048$

$a = 40$ ft $\qquad D = \frac{d}{a} = 0{\cdot}125$

$d = 5$ ft $\qquad r = \frac{a}{L} = 0{\cdot}8$

$2b = 0{\cdot}82$ ft $\qquad h = \frac{t}{2a} = 0{\cdot}0015625$

$2t = 0{\cdot}25$ ft

$\phi_o = 40°$

A minimum value for P_u is obtained from the velocity field I, case (i). Using equations (11) and (12),

$$P_u = 0{\cdot}225$$

The lower bound for this shell, worked out in a previous paper[6], is

$$P_L = 0{\cdot}0931$$

Acknowledgments

The authors are grateful to Professor G. S. Ramaswamy for his encouragement and suggestions in the preparation of this paper.

This paper is published with the permission of the Director, Central Building Research Institute, Roorkee.

References

1. Fialkow, M. N. "Limit analysis of simply supported circular shell roofs". *Jour. Eng. Mech. Div., Am. Soc. C. E.*, July 1958. pp. 1706 (1–39).
2. Baker, A. L. L. "A plastic design theory for reinforced and prestressed concrete shell roofs". *Mag. Concrete Research*, 1950. No. 4, pp 27–34.
3. Johansen, K. W. "Critical notes on calculation and design of cylindrical shells". Proc., Third Congress, International Association for Bridge and Structural Engineering, 1948, pp 601–606.
4. Sawczuk, A. "On experimental foundations of limit analysis theory of reinforced concrete shells". Proc. Symposium on Shell Research, Delft, 1961. pp 217–231.
5. Hill, R. Progress in Solid Mechanics, Vol II. North Holland Publishing Co, 1961. pp 247–276.
6. Keshava Rao, M. N. and Raman, N. V. "Lower Bounds for collapse loads of cylindrical shells with edge beams". *The Indian Concrete Journal*, November 1963. Vol. 37. pp 402–6.
7. Hodge, P. G. Plastic Analysis of Structures. McGraw Hill Book Co, New York, 1959.

Printed by Pyarelal Sah at The Times of India Press, Bombay, India, and published by M. H. Engineer, B.A., B.Com., for the Cement Marketing Co. of India Ltd. at 'Cement House', 121, Queen's Road, Bombay.